Dynamical constraints and signals of phase transition

Münster University of Applied Sciences

Klaus Morawetz

International Institute of Physics
Federal University of Rio Grande do Norte

1. Non-local kinetic theory
   - Quantum correlation recast into nonlocal shifts, consistent conserving theory
   - Unification theory of dense classical gases with Landau Fermi liquid
2. Nuclear collisions at Fermi energy
   - Enhancement of midrapidity distribution and neck fragmentation
   - anomalous velocity profiles, non - Hubblean expansion, squeezing modes
   - Nonequilibrium thermodynamics iso-nothing plots
3. Critical summary: equation of state if no states?

Forschungszentrum Dresden Rossendorf | Chemnitz University | MPI for the Physics of Complex Systems | LPC/ISMRA | Catania | Arizona State University | Michigan State University | Tennessee Tech University | Rostock University

Saturation properties: 2- and 3-particle correlational energy

Hartree-Fock mean field Skyrme

$$\frac{E}{A} = \frac{\mathcal{E}}{n} = \frac{3}{5}\epsilon_f + \frac{3}{8}t_0 n + \frac{1}{16}t_3 n^2$$

Galitskii 2-particle correlational energy

$$\begin{aligned}\frac{E_{\mathrm{corr}_2}}{n} &= 4\epsilon_f \frac{2\log 2 - 11}{35}\left(\frac{p_f m T_2}{4\pi^2\hbar^3}\right)^2 \\ &= -\frac{5.7910^{-5}}{\mathrm{MeV\,fm}^2} n^{4/3}\left[9{t_0}^2 + \frac{3}{4}{t_3}^3 n^2 + 5 t_3 t_0 n\right]\end{aligned}$$

3-particle correlational energy (7-fold integral)

$$\begin{aligned}\frac{E_{\mathrm{corr}_3}}{n} &= 4\epsilon_f \frac{9013}{2\cdot 9\cdot 25\cdot 77\cdot 13}\left(\frac{p_f^4 m T_3}{4\pi^4\hbar^6}\right)^2 \\ &= \frac{2.3710^{-6}}{\mathrm{MeV\,fm}^2} n^{10/3}{t_3}^2\end{aligned}$$

K. Morawetz PRC 63 (2000) 014609

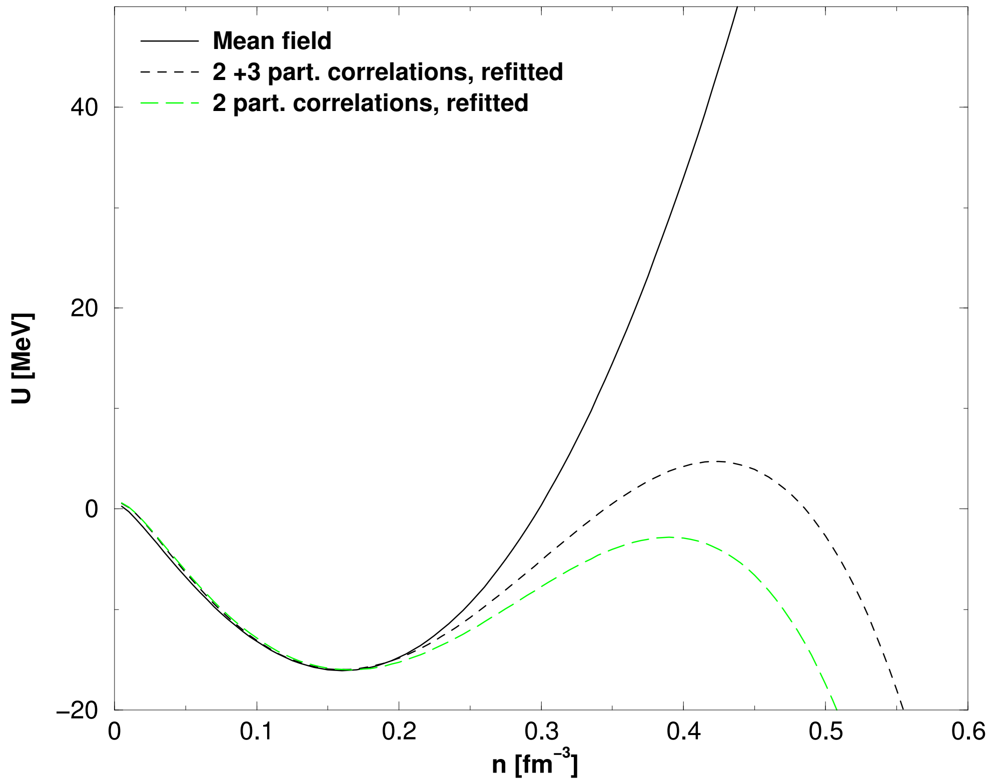

Relative importance

$$\left|\frac{E_2}{E_3}\right| = \frac{2^5\cdot 5\cdot 11\cdot 13}{9013}(11 - 2\log 2)\left[9\frac{{t_0}^2}{n^2{t_3}^2} + \frac{3}{4} + 5\frac{t_0}{t_3 n}\right]$$

decreasing with minimal ratio 1.4 at $n_{\min} == 0.32\mathrm{fm}^{-3}$

higher densities: 18.3

Nonlocal kinetic theory

$$\frac{\partial f_1}{\partial t}+\frac{\partial \varepsilon_1}{\partial k}\frac{\partial f_1}{\partial r}-\frac{\partial \varepsilon_1}{\partial r}\frac{\partial f_1}{\partial k}=\sum_{pq}\left[\mathcal{P}^-\left(1-f_1-f_2^-\right)f_3^-f_4^- - \mathcal{P}^\mp f_1 f_2^\mp\left(1-f_3^\mp-f_4^\mp\right)\right]$$

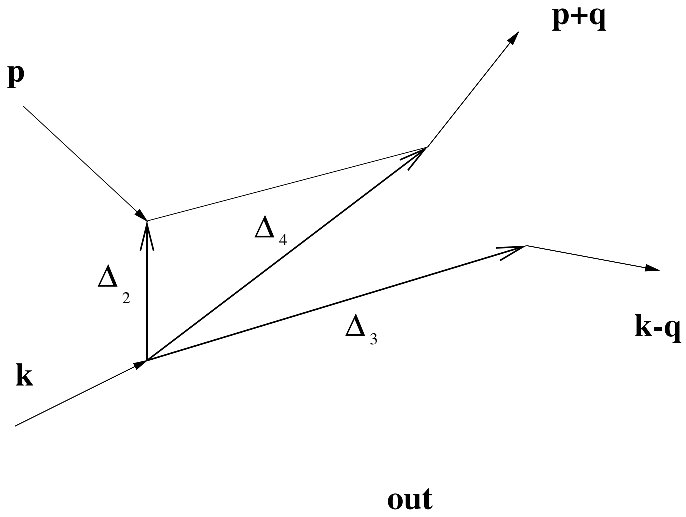

$\mathcal{P}^\mp=\delta\left(\varepsilon_1+\varepsilon_2^\mp-\varepsilon_3^\mp-\varepsilon_4^\mp-2\Delta_E\right)|T^\mp|^2$ with T-matrix

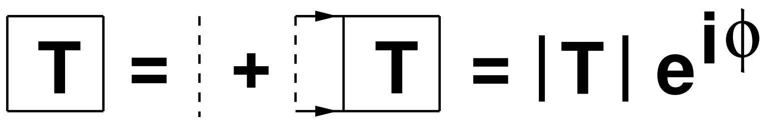

and shifts

$$\Delta_t = \left.\frac{\partial \phi}{\partial \Omega}\right|_{\varepsilon_1+\varepsilon_2} \qquad \Delta_2 = \left(\frac{\partial \phi}{\partial p}-\frac{\partial \phi}{\partial q}-\frac{\partial \phi}{\partial k}\right)_{\varepsilon_1+\varepsilon_2}$$

$$\Delta_E = -\left.\frac{1}{2}\frac{\partial \phi}{\partial t}\right|_{\varepsilon_1+\varepsilon_2} \qquad \Delta_3 = -\left.\frac{\partial \phi}{\partial k}\right|_{\varepsilon_1+\varepsilon_2}$$

$$\Delta_K = \left.\frac{1}{2}\frac{\partial \phi}{\partial r}\right|_{\varepsilon_1+\varepsilon_2} \qquad \Delta_4 = -\left(\frac{\partial \phi}{\partial k}+\frac{\partial \phi}{\partial q}\right)_{\varepsilon_1+\varepsilon_2}$$

where

$$\begin{aligned} f_1 &\equiv f(k,r,t)\\ f_2^- &\equiv f(p,r-\Delta_2,t)\\ f_3^- &\equiv f(k-q-\Delta_K,r-\Delta_3,t-\Delta_t)\\ f_4^- &\equiv f(p+q-\Delta_K,r-\Delta_4,t-\Delta_t)\end{aligned}$$

P. Lipavský, K. Morawetz, and V. Špička: Annales de physique, 26,1 (2001) ISBN 2-86883-541-4
Realistic shifts: K. Morawetz, P. Lipavský, V. Spicka, N. H. Kwong, PRC 59 (1999) 3052

Nonlocal shifts with realistic potentials

K. Morawetz, P. Lipavsky, V. Spicka, and N.-H. Kwong, Phys. Rev. C 59, 3052 (1999)

The shifts correspond to classical parameter

$$\Delta_\phi = \alpha|\cos\frac{\theta}{2}|\frac{\vec\kappa+\vec\kappa_f}{|\vec\kappa+\vec\kappa_f|}$$

$$\Delta_{\rm HS} = 2d|\sin\frac{\theta}{2}|\frac{\vec\kappa-\vec\kappa_f}{|\vec\kappa-\vec\kappa_f|}$$

$$\Delta_f = \Delta_t\frac{\vec K}{m_a+m_b}$$

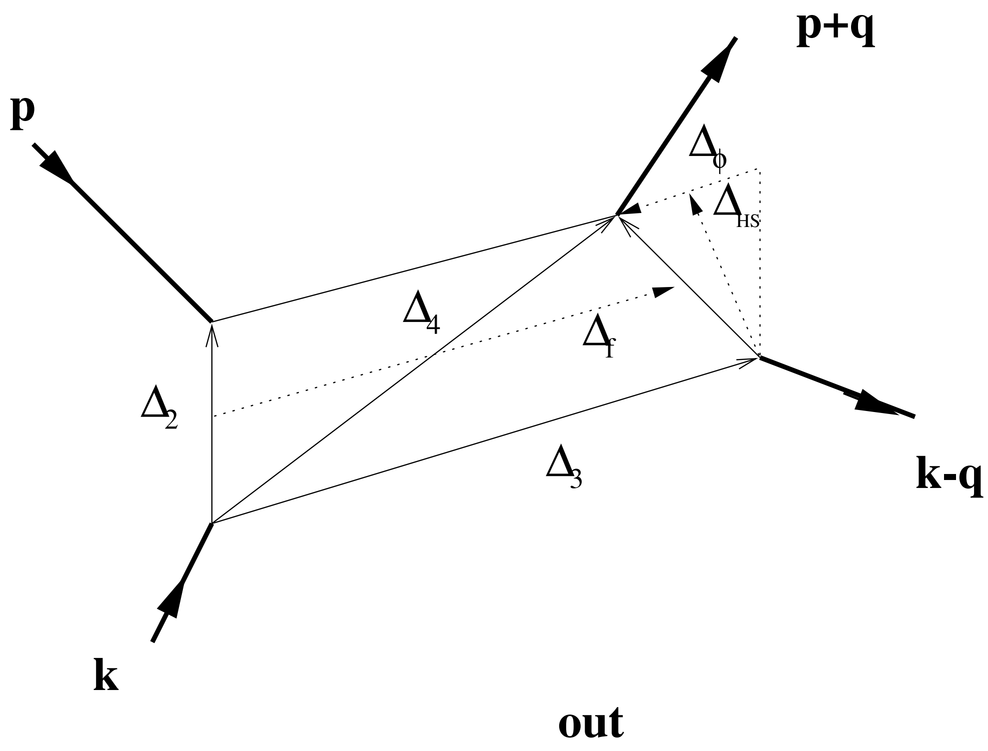

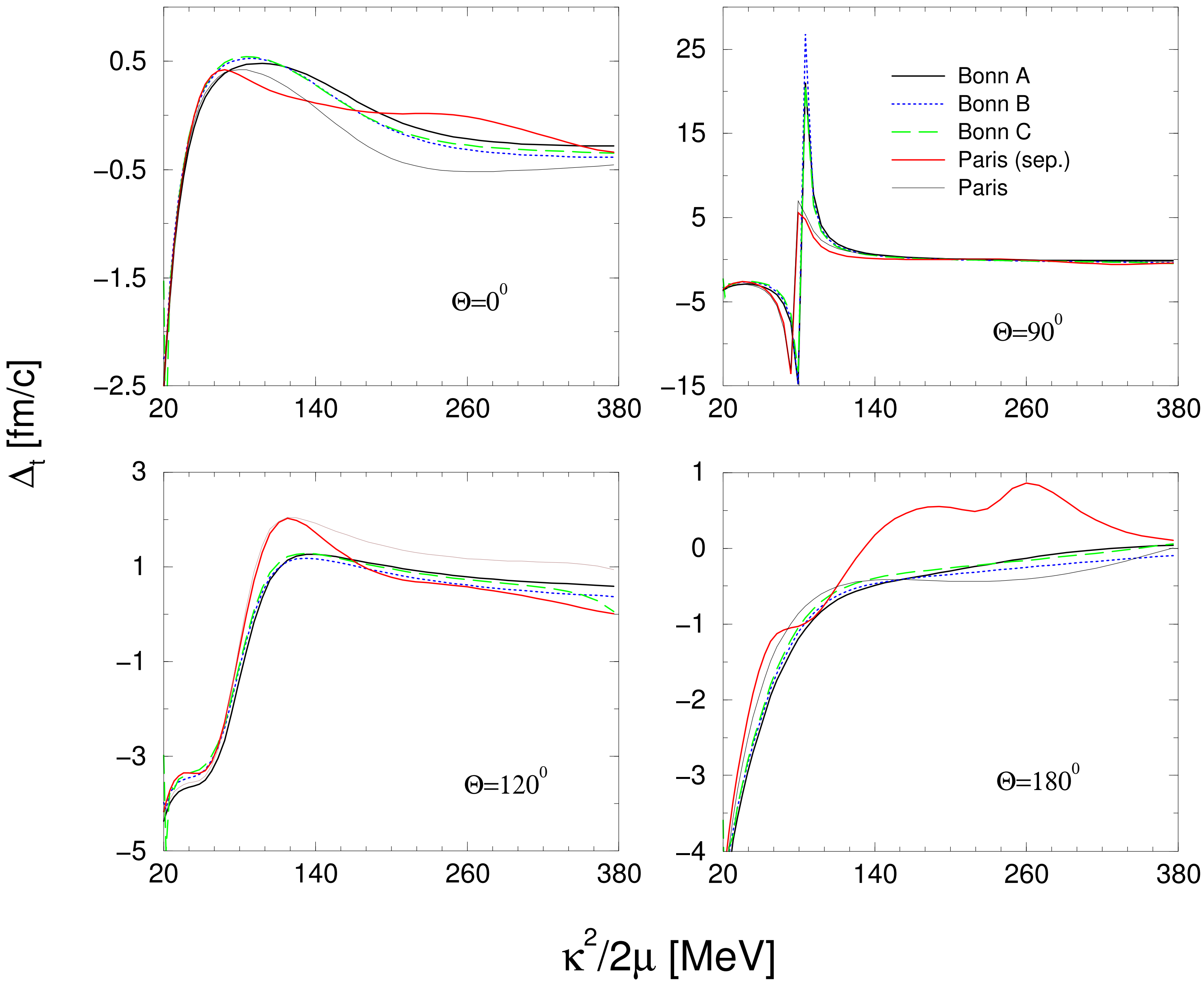

The time delay versus lab energies for different scattering angles.

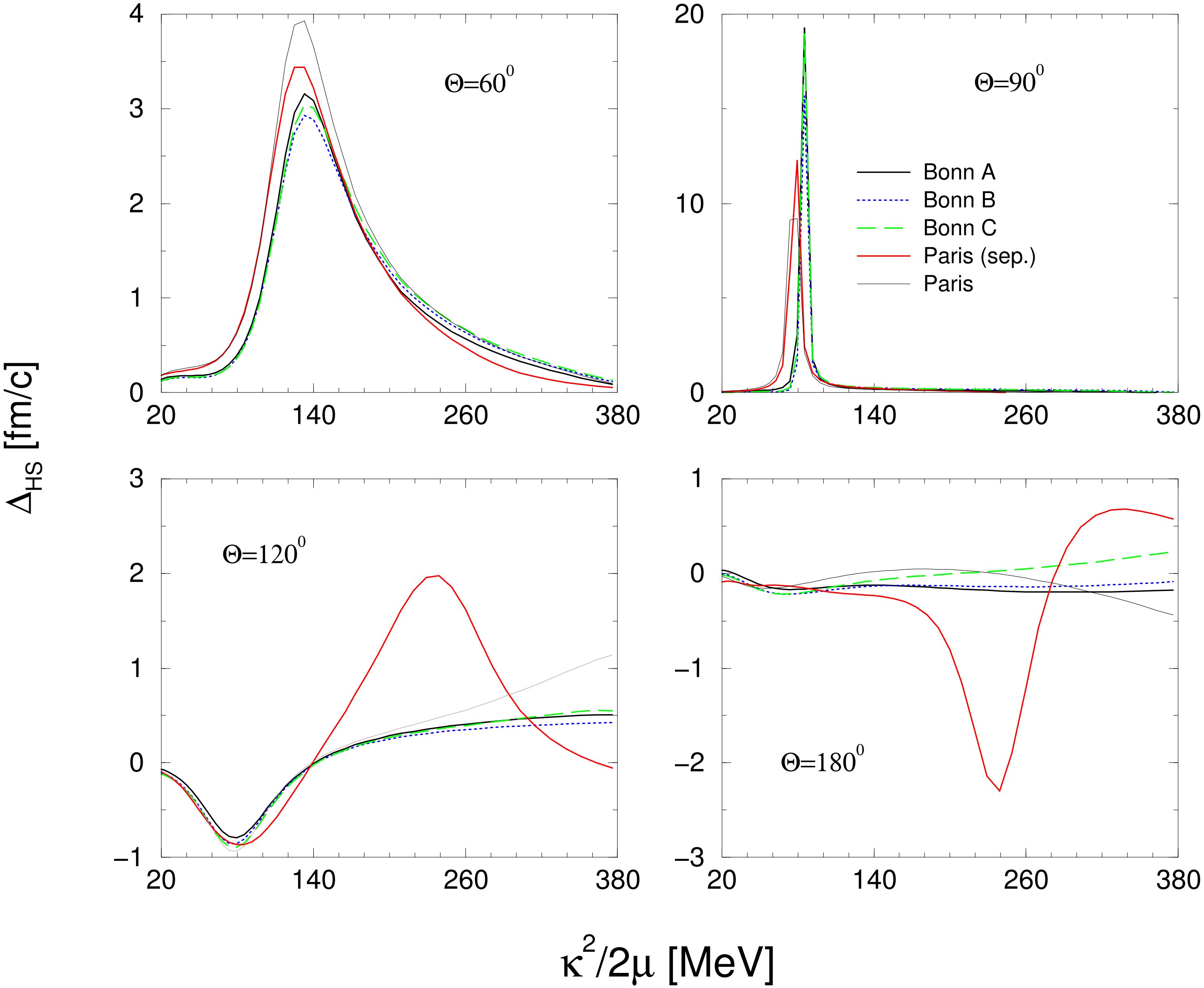

The Enskog displacement parameter d versus lab energies.

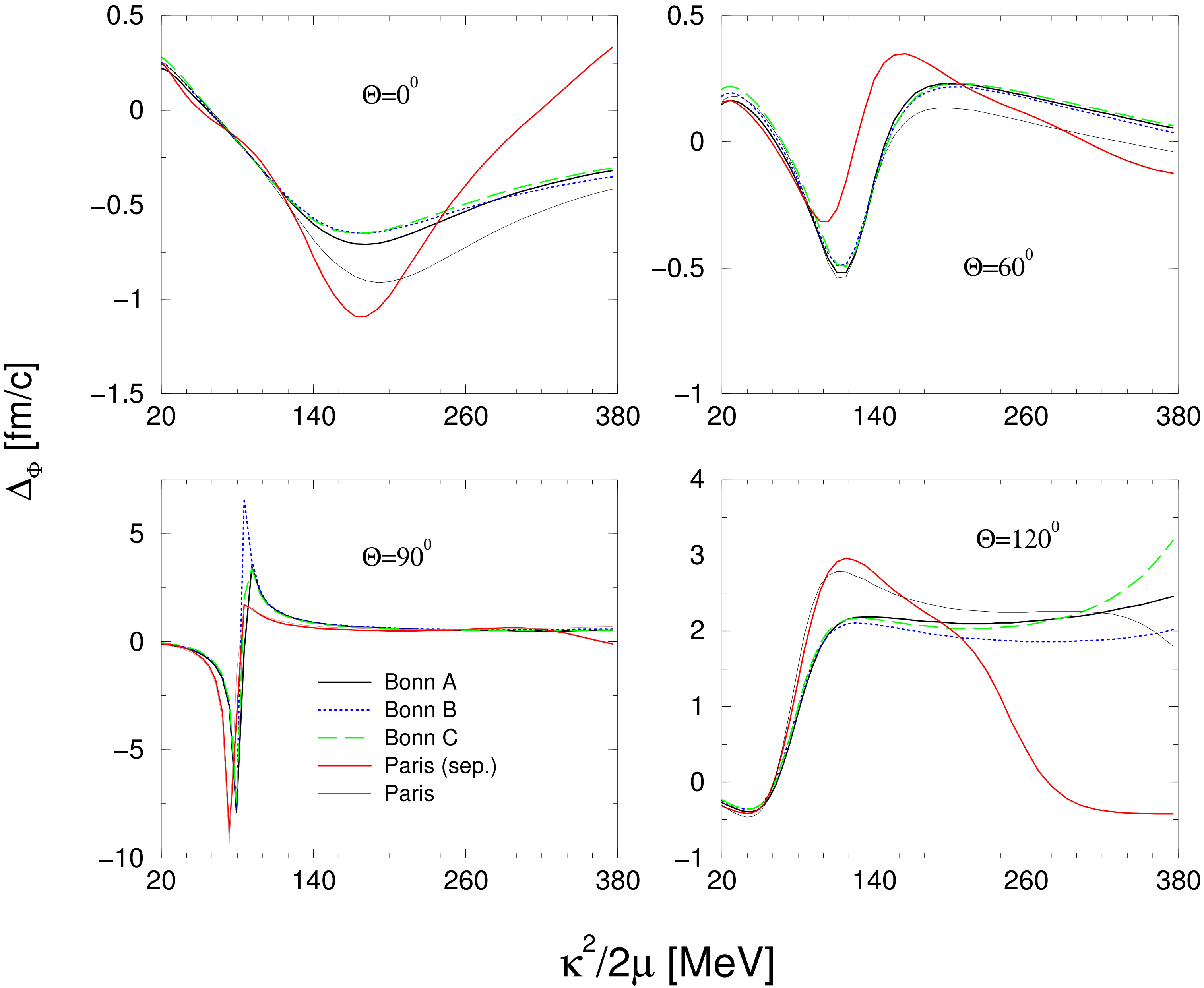

The molecule rotation displacement α versus lab energies.

$Ta + Au$ collisions at $E_{lab}/A = 33$ MeV and 8fm impact parameter

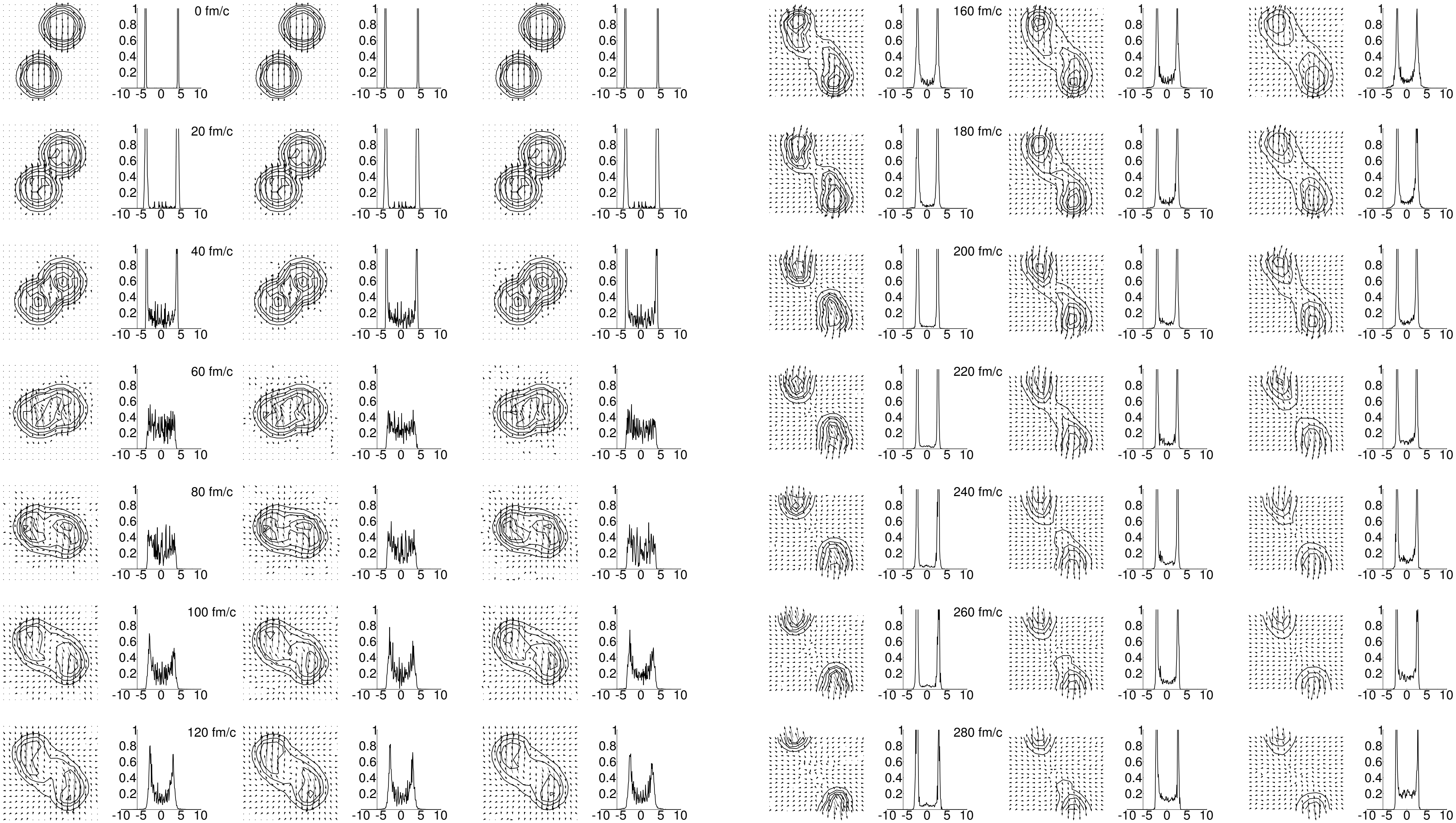

BUU (left), nonlocal (middle), nonlocal with quasiparticle renormalizations (right)

x, y - density cuts, charge density distribution vs. relative velocity [cm/ns].

Charge distribution vs. velocity $Ta + Au$ at 33 MeV

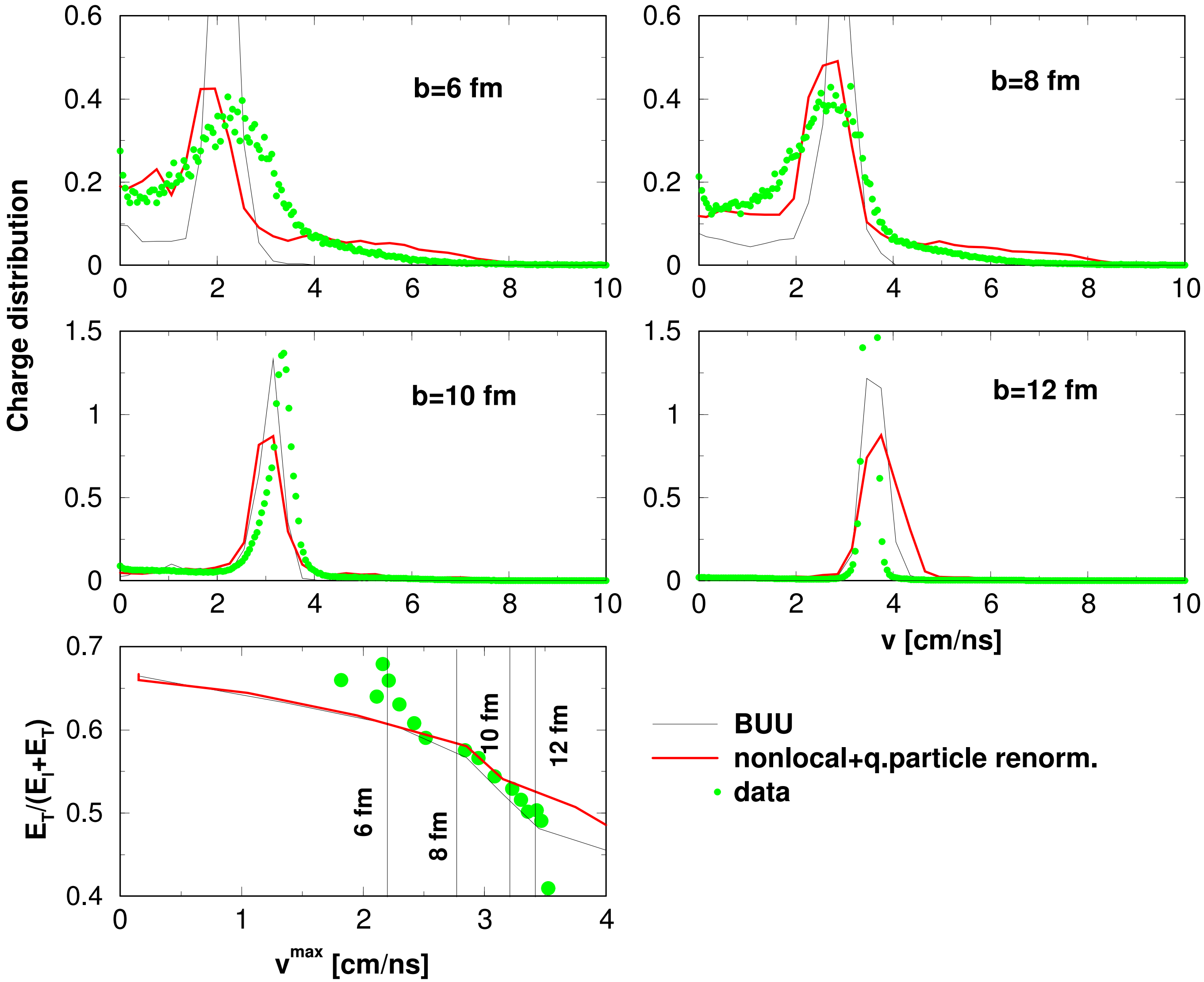

Experimental charge distribution vs. velocity with BUU and the nonlocal model with quasiparticle renormalizations cuts by maximum velocity vs. ratio of longitudinal to total kinetic energy

K. Morawetz, P. Lipavsky, J. Normand, D. Cussol, J. Colin, B. Tamain
PRC 63 (2001) 034619

Central collision Sn+Sn at 50MeV

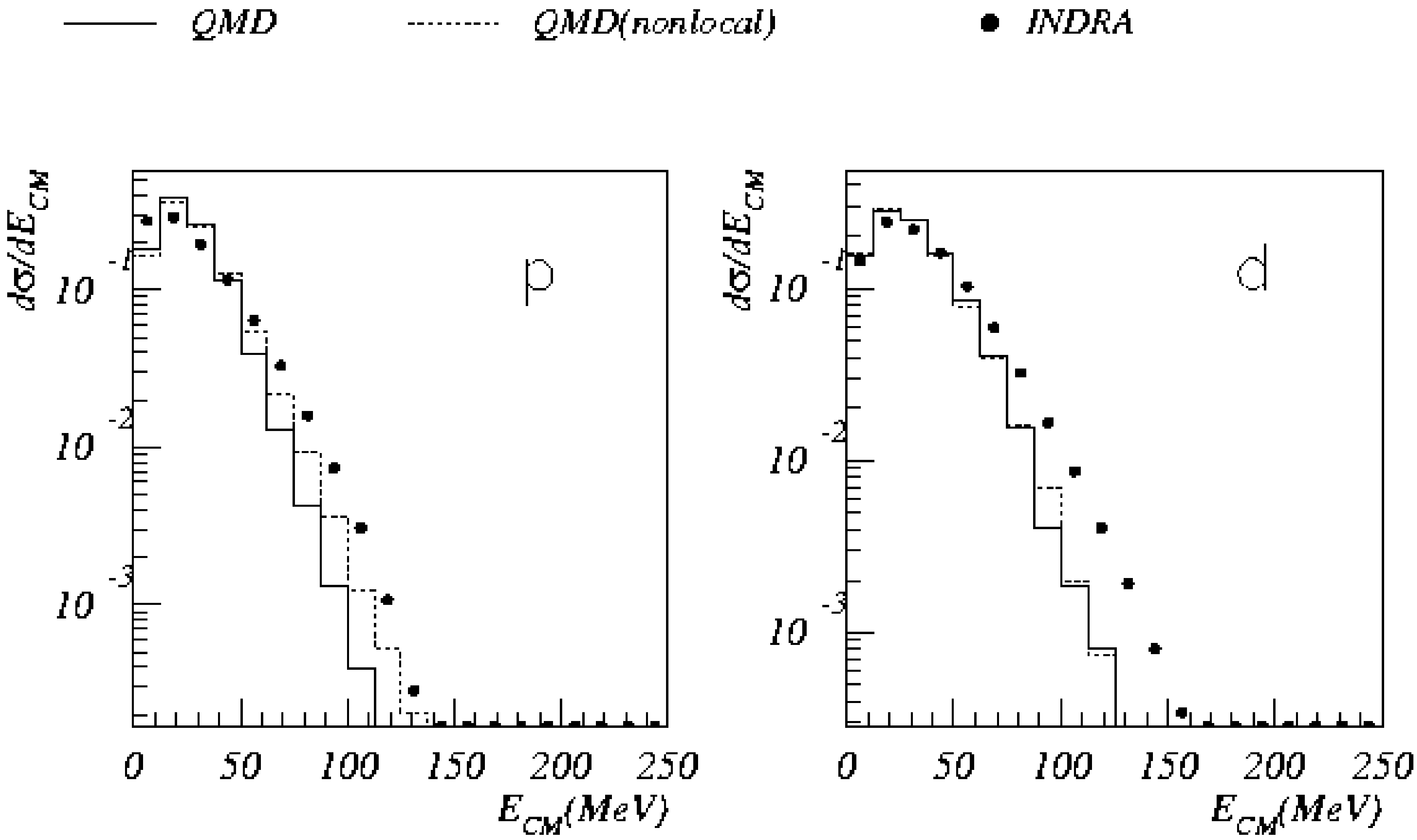

Simulation: modified QMD code of J.Aichelin
K. Morawetz, V. Spicka, P. Lipavsky, G. Kortemeyer, Ch. Kuhrts, R. Nebauer
PRL 82 (1999) 3767

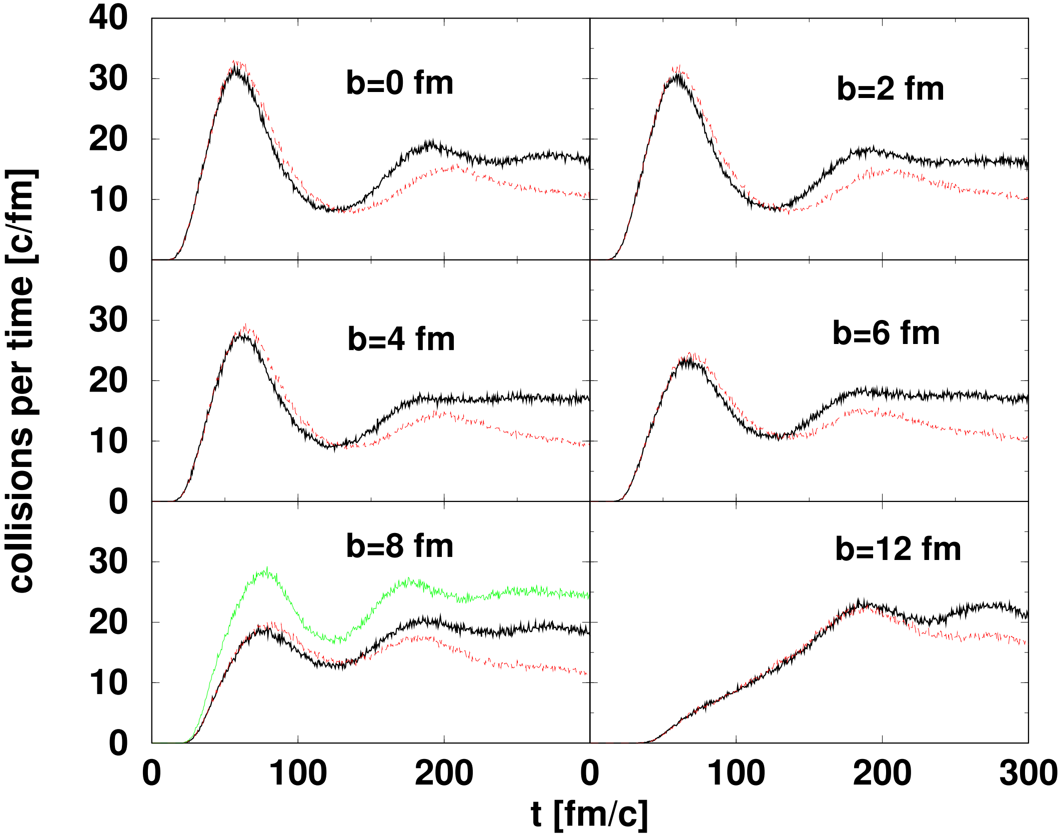

Number of collisions

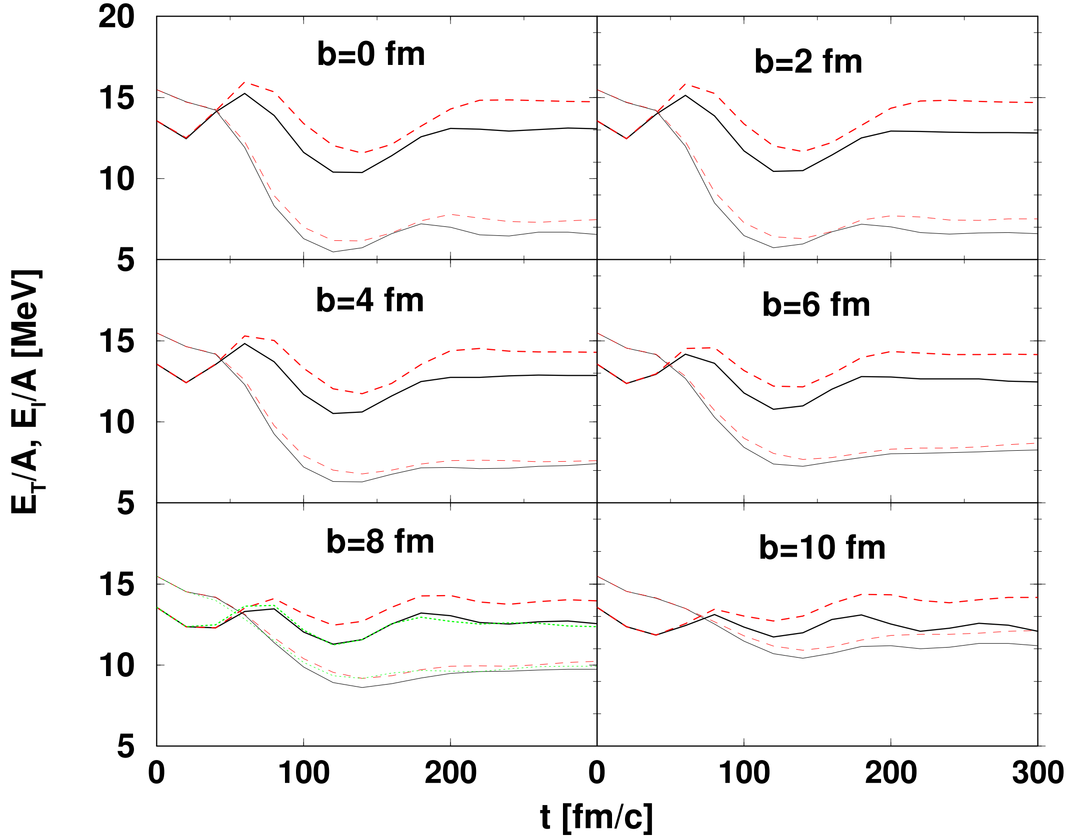

Longitudinal (lower), transverse (upper) energy

BUU (thick black line), nonlocal, local BUU but twice cross section (green line)

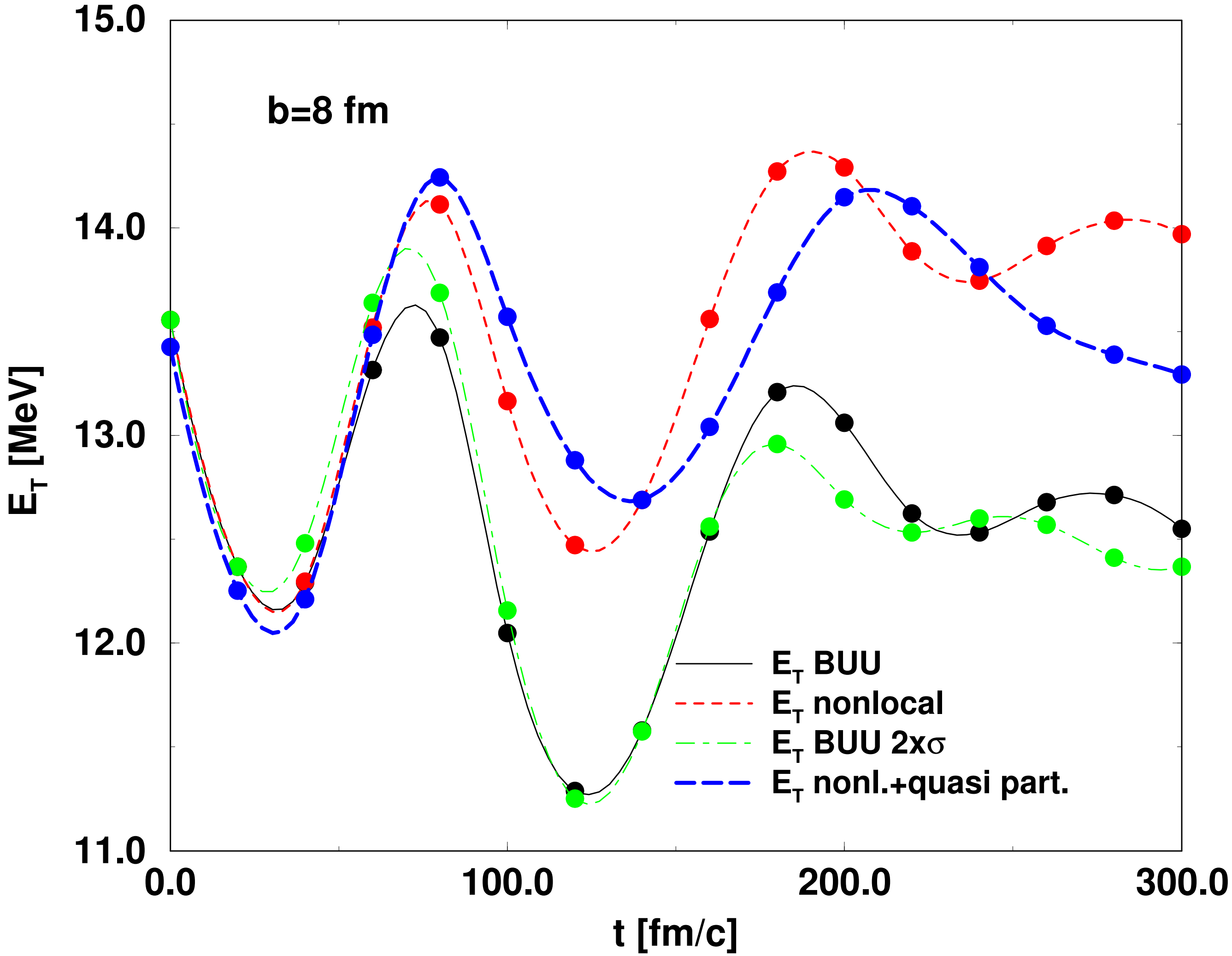

transverse energy BUU, nonlocal, local BUU but twice cross section and the nonlocal scenario with quasiparticle renormalization (long dashed line)

Radial dependence of velocity and density

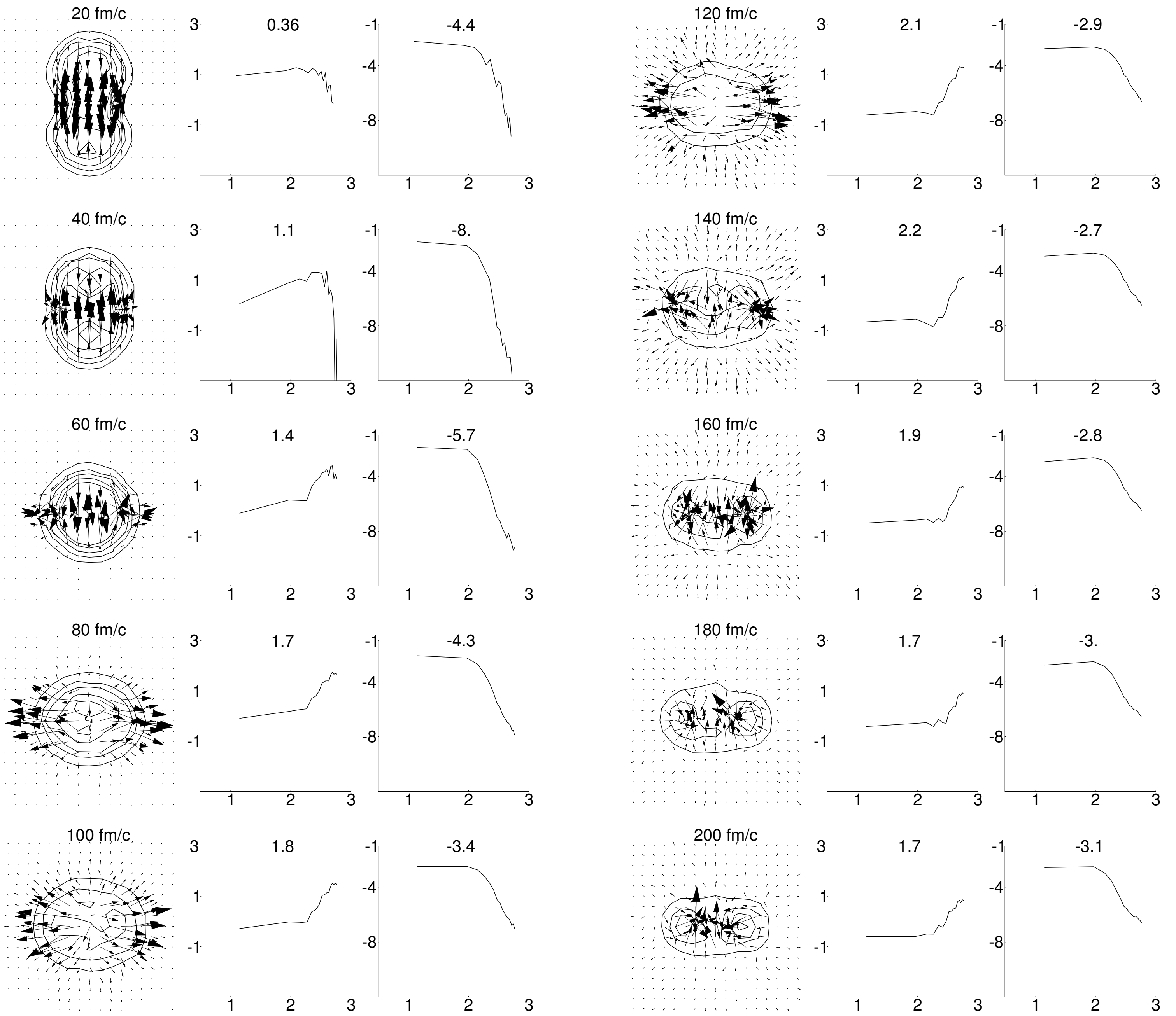

central $Ta + Au$ at $E_{lab}/A = 33$ MeV

density cuts mass momenta by arrows

log - log plot of angular averaged modulus of expansion velocity and density vs. radius

slope of surface matter for $R > 10$ fm

Radial dependence of velocity and density

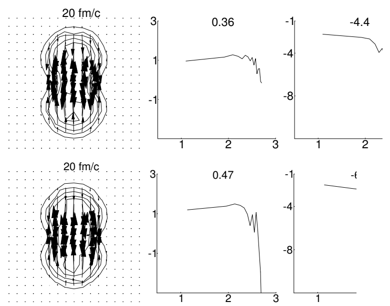

$v \propto r^{\alpha}$

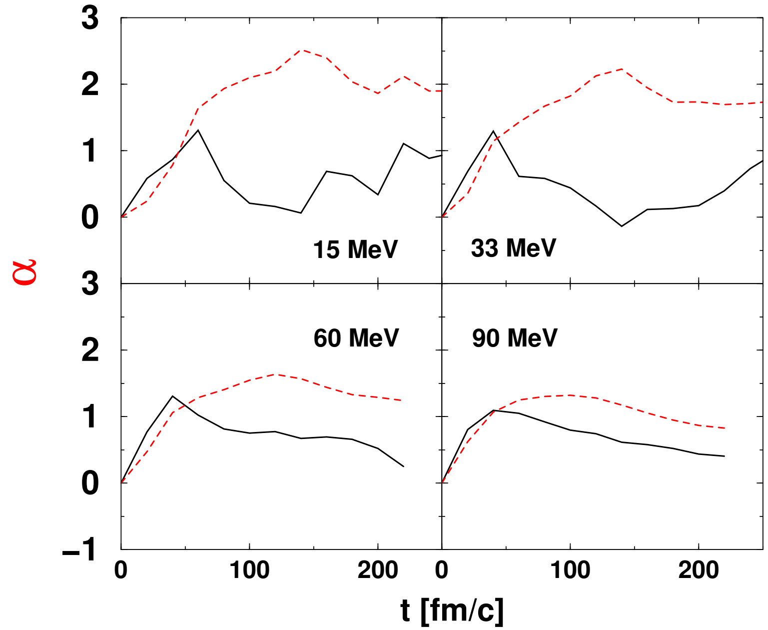

surface matter, bulk matter

$n \propto r^{-\beta}$

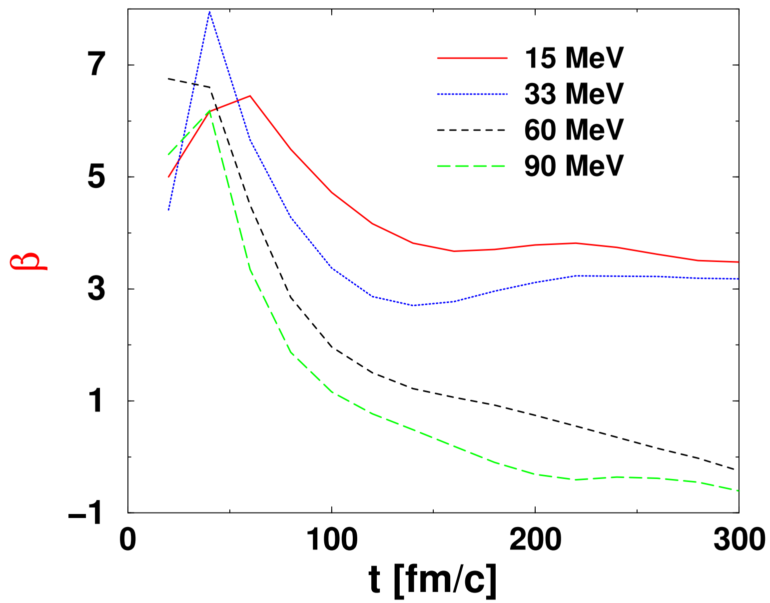

surface region ($R > 10$ fm)

Hubble expansion: total energy h of radially symmetric matter $\frac{m}{2}\dot{R}(t)^2 - \frac{G}{R(t)^{\delta}} = h$

homogeneous density n, escaping matter $(h = 0)$ means $\dot{R}(t) = \sqrt{\frac{6G}{4\pi n}} R(t)^{\frac{3-\delta}{2}}$

$\alpha = \frac{3-\delta}{2} = 1$ corresponds to $\delta = 1$ (Coulomb, Gravitation), $\alpha = 2$ corresponds to $\delta = -1$ (String force)

Universal Fluctuations Xe+Sn

Δ −scaling : $$< m >^{\Delta} P_{<m>}[m] = \Phi\left(\frac{m - m^*}{< m >^{\Delta}}\right)$$

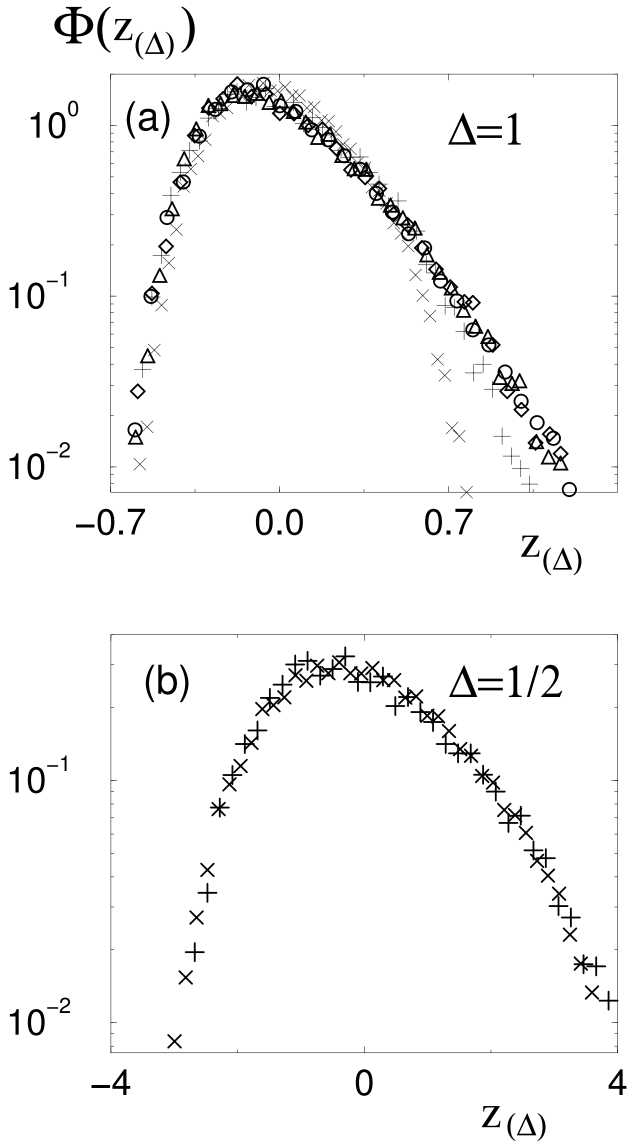

$\kappa_1 =< m >$, $\kappa_2 =< m^2 > - < m >^2$, $K_2 = \kappa_2/\kappa_1^2$

R. Botet, M. Płoszajczak, A. Chbihi, B. Broderie, D. Durand, J. Frankland, PRL86 (2001) 3514

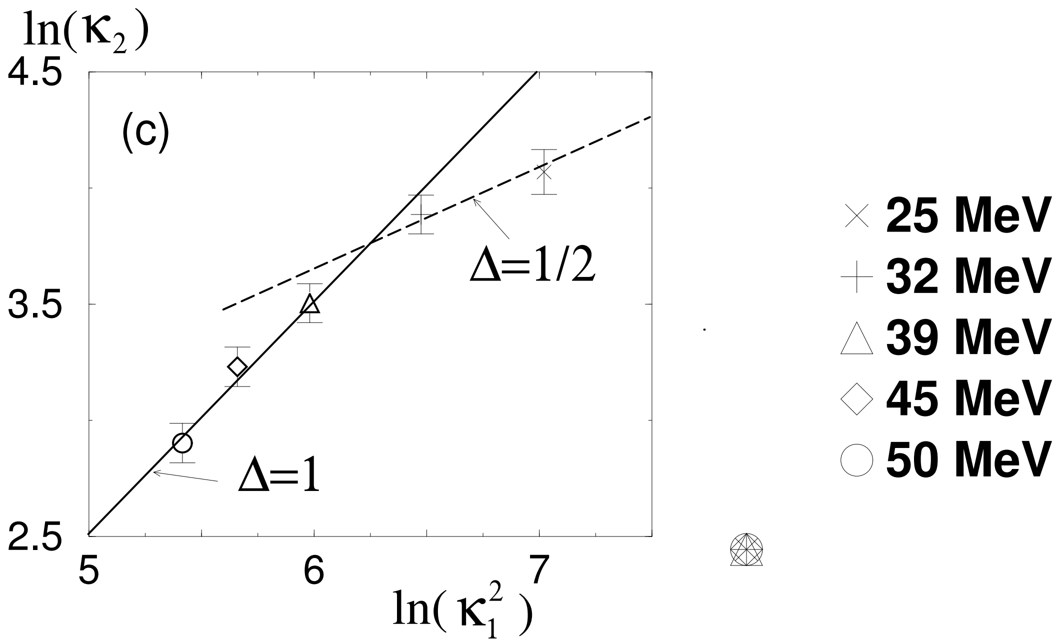

predicted: K. Morawetz: PRC 62 (2000) 044606

K. M., M. Płoszajczak, V.D. Toneev: PRC 62 (2000) 064602

Interpretation in terms of Tsallis statistics $n \sim r^{-3}$, $v \sim r^2$

D. Prato and C. Tsallis, Phys. Rev. E 60 (1999) 2398

$$\frac{\partial}{\partial t} P(x,t) = D \nabla^{\gamma} P(x,t)^{\nu}$$

Anomalous Diffusion
M. Bologna, C. Tsallis, and P. Grigolini,
Phys. Rev. E 62 (2000) 2213

$$\lim_{\gamma \to 2} P(x,t,\gamma) \propto x^{-3} \qquad q = \frac{\gamma+3}{\gamma+1} \approx \frac{5}{3}$$

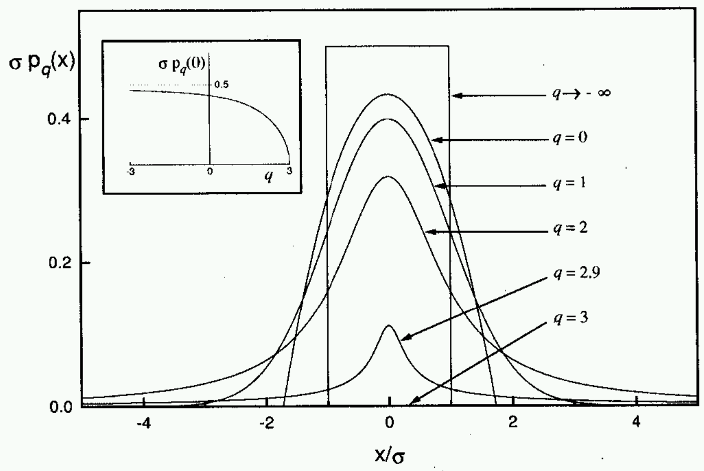

FIG. 1. The one-jump distributions $p_q(x)$ for typical values of q. The $q \to -\infty$ distribution is the uniform one in the interval $[-1,1]$; $q=1$ and $q=2$, respectively, correspond to Gaussian and Lorentzian distributions; the $q \to 3$ distribution is completely flat. For $q<1$, there is a cutoff; for $q>1$, there is a $1/|x|^{2/(q-1)}$ tail at $|x| \gg \sigma$.

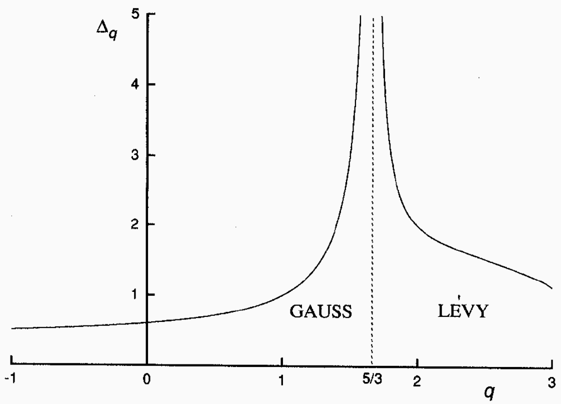

FIG. 2. The q dependence of the dimensionless diffusion coefficient Δ_q [*width* of the properly scaled distribution $p_q(x,N)$ in the $N \to \infty$ limit]. In the limits $q \to 5/3 - 0$ and $q \to 5/3 + 0$ we, respectively, have $\Delta_q \sim [4/9]/[(5/3) - q]$ and $\Delta_q \sim [4/(9\pi^{1/2})]/[q - (5/3)]$; also, $\lim_{q \to 3} \Delta_q = 2/\pi^{1/2}$.

$$v(r) \approx \langle x \dot{P}(x,t) \rangle \propto \frac{1}{b^2} \approx \frac{1}{b^2} + \frac{z^2}{2} + o(bz^3)$$

K. Morawetz, Physica A 305 (2002) 234

Squeezing mode $Ta + Au$ at 33 MeV and 8 fm impact

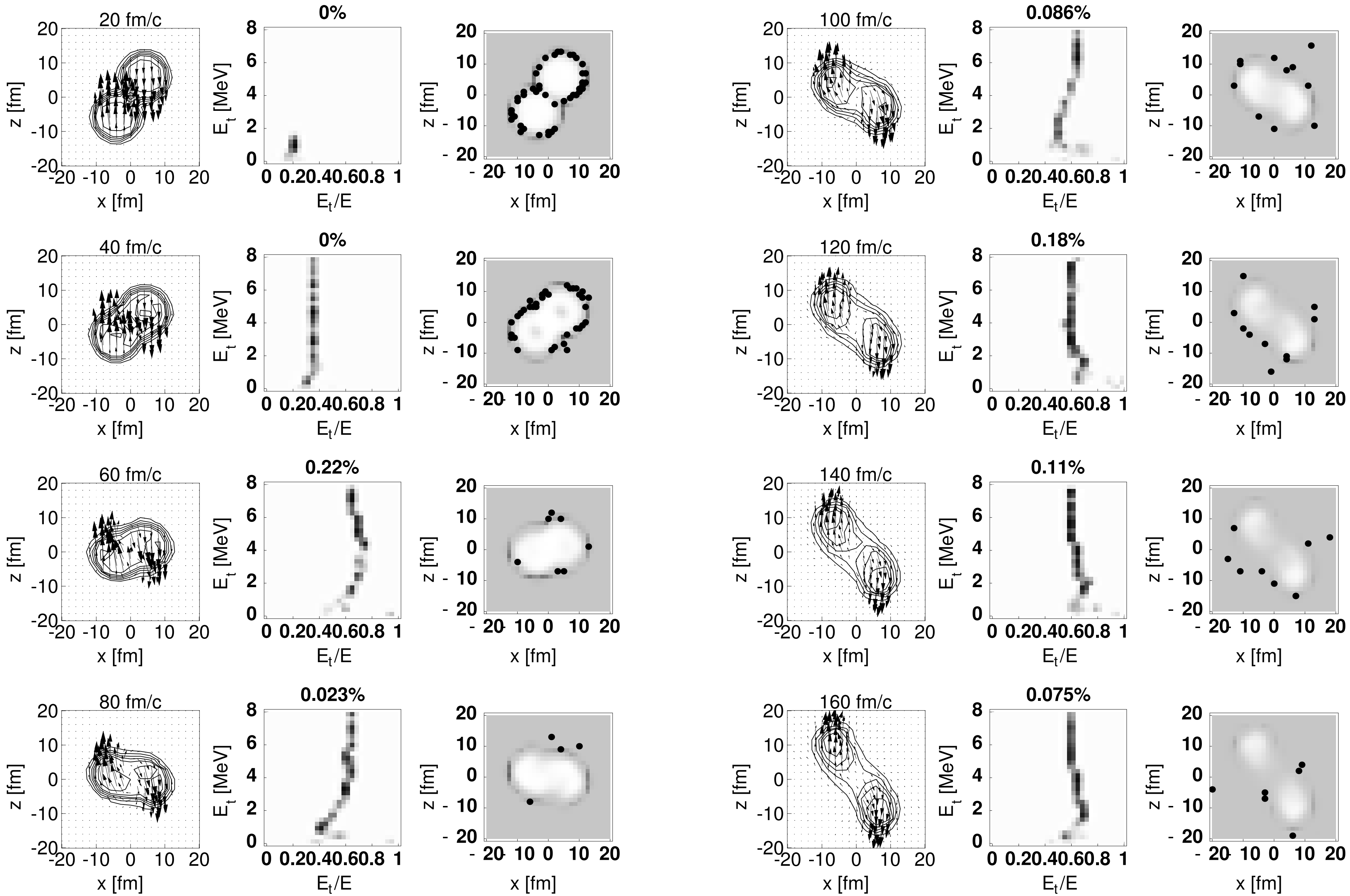

left: density and currents; middle: trans. energy vs. trans./total; right: dark $E > 0$ escape, light $E < 0$

K. Morawetz, P. Lipavsk'y, PRC 63 (2001) 061602(R)

Nonequilibrium Thermodynamics

From distribution function local quantities (densities)

$$\begin{matrix} \text{number} & n(\mathbf{r},t) \\ \text{current} & \mathbf{J}(\mathbf{r},t) \\ \text{kin. energy} & E_K(\mathbf{r},t) \end{matrix} = \sum_p \begin{pmatrix} 1 \\ \mathbf{p} \\ \frac{p^2}{2m} \end{pmatrix} f(\mathbf{p},\mathbf{r},t)$$

Global variables/particle by spatial integration

$$\text{kin. energy} \quad E_K(t) = \int d\mathbf{r} E_K(\mathbf{r},t)$$

$$\text{Fermi energy} \quad E_F(t) = \int d\mathbf{r} E_f[n(\mathbf{r},t)]n(\mathbf{r},t) \Big/ \int d\mathbf{r} n(\mathbf{r},t)$$

$$\text{coll. energy} \quad E_{\text{coll}}(t) = \int d\mathbf{r} \frac{J(\mathbf{r},t)^2}{mn(\mathbf{r},t)} \Big/ \int d\mathbf{r} n(\mathbf{r},t)$$

$$\text{Meanfield} \quad U(t) = \int d\mathbf{r} \left(\frac{an^2}{2n_0} + \frac{bn^{s+1}}{(s+1)n_0^s} \right) \Big/ \int d\mathbf{r} n(\mathbf{r},t)$$

$$\text{Bin. corr energy} \quad E_2(t) = E_F^2 \frac{2Ln2-11}{70\pi^3} \frac{m}{\hbar^2} \sigma + o(T^3)$$

Temperature-independent plots

Fermi liquid temperature $E_K(t) = \frac{3}{5}E_F(t) + E_{\rm coll}(t) + \frac{\pi^2}{4E_F(t)}T(t)^2$

Pressure/particle

$$P = \frac{2}{3}(E_K(t) - E_{\rm coll}(t)) + \frac{4}{3}E_2(t) + \int d\mathbf{r}\left(\frac{an}{2n_0} + \frac{bsn^s}{(s+1)n_0^s}\right) \Big/ \int d\mathbf{r}\, n(\mathbf{r},t)$$

"Energy" : $E(t) = E_K(t) - E_{\rm coll}(t) + U(t)$

Equilibrium spinodal: temperature independent plot iso -nothing

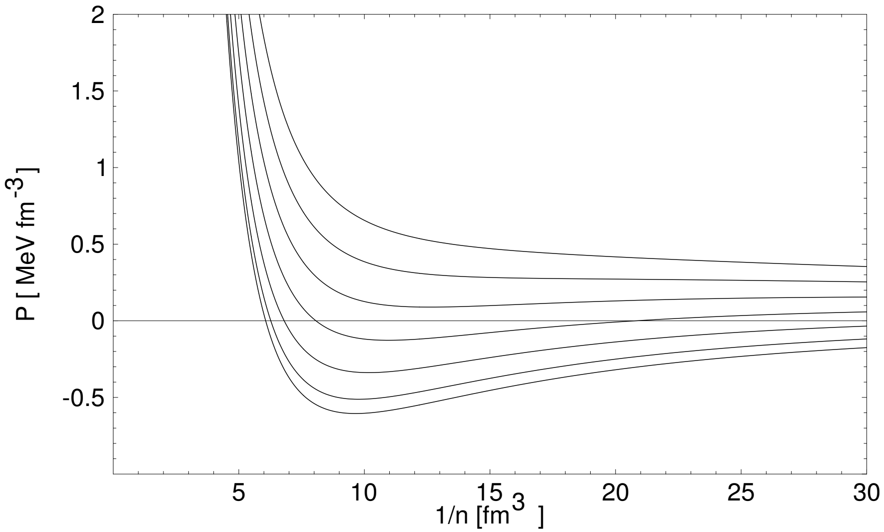

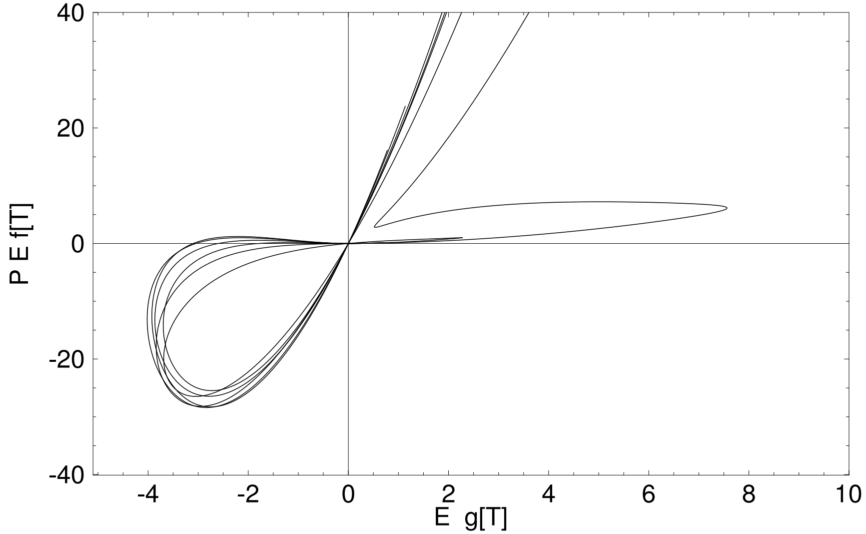

K. Morawetz Phys. Rev. C 62, 44606 (2000)

Dynamical trajectories

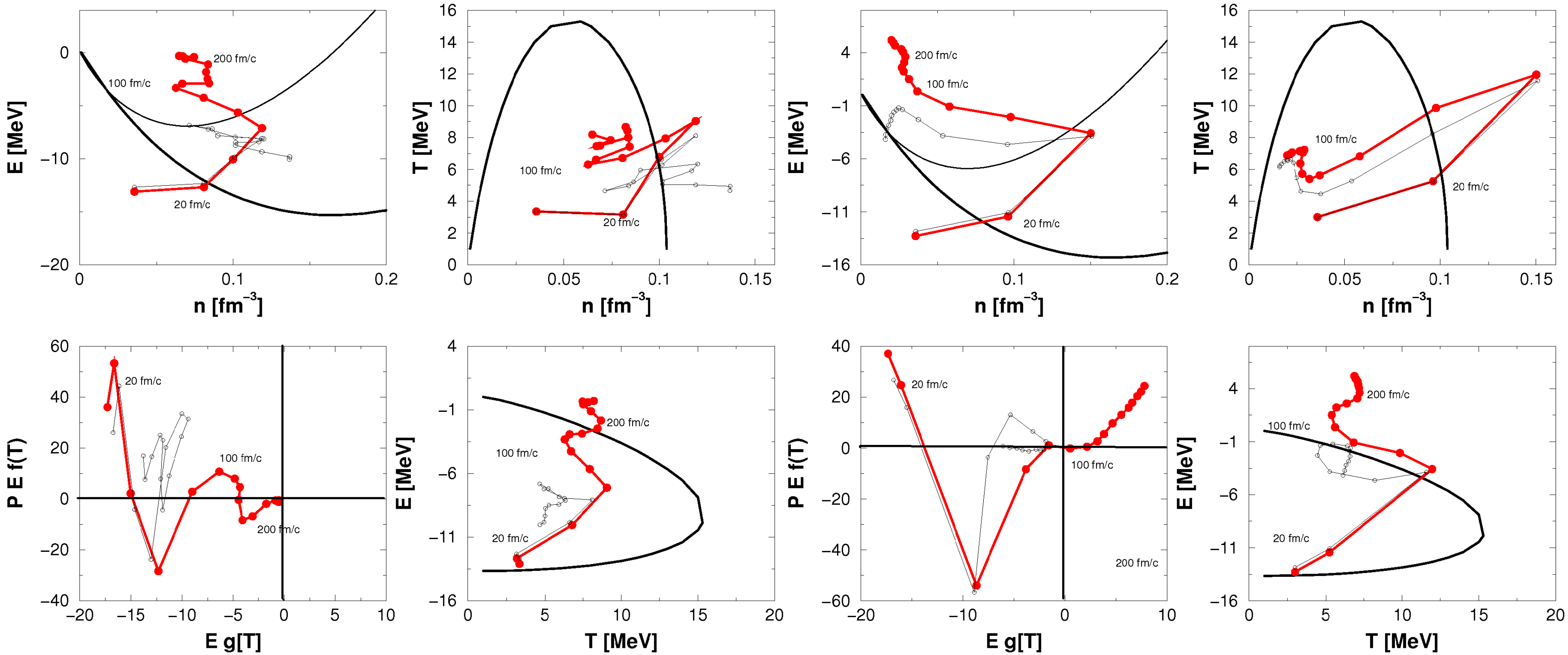

Dynamical trajectories in nonlocal and local BUU (black) scenario for ^{129}Xe on ^{119}Sn at 25 and 50MeV lab energy, times steps from 20fm/c to 300fm/c

zero temperature mean field energy (thick line) and the pressure (thin line) in upper left picture, temperature-independent plot in lower left

25MeV

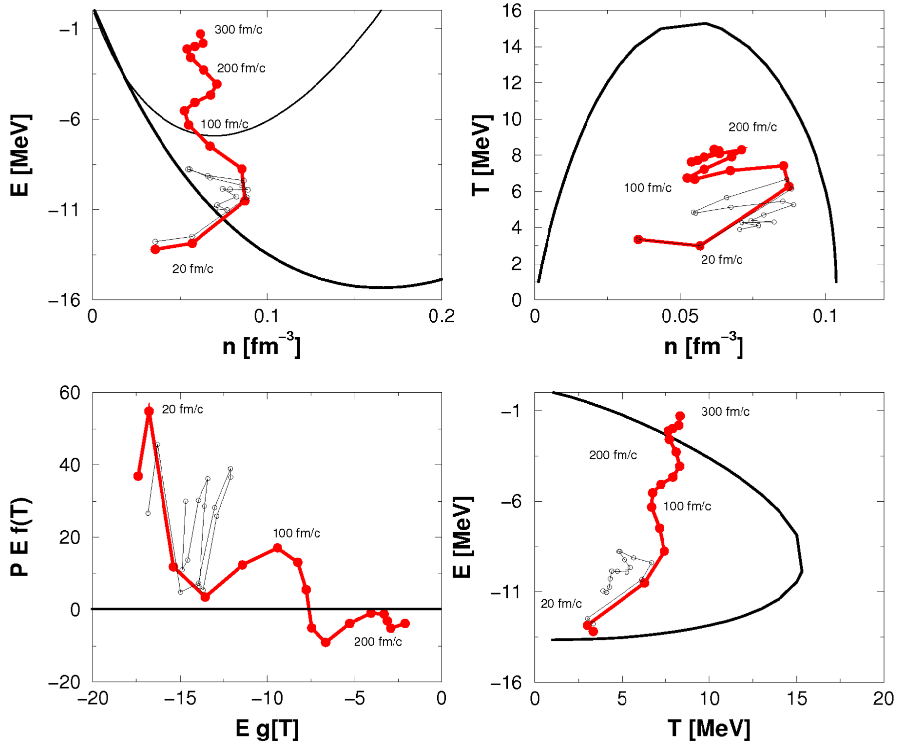

50MeV

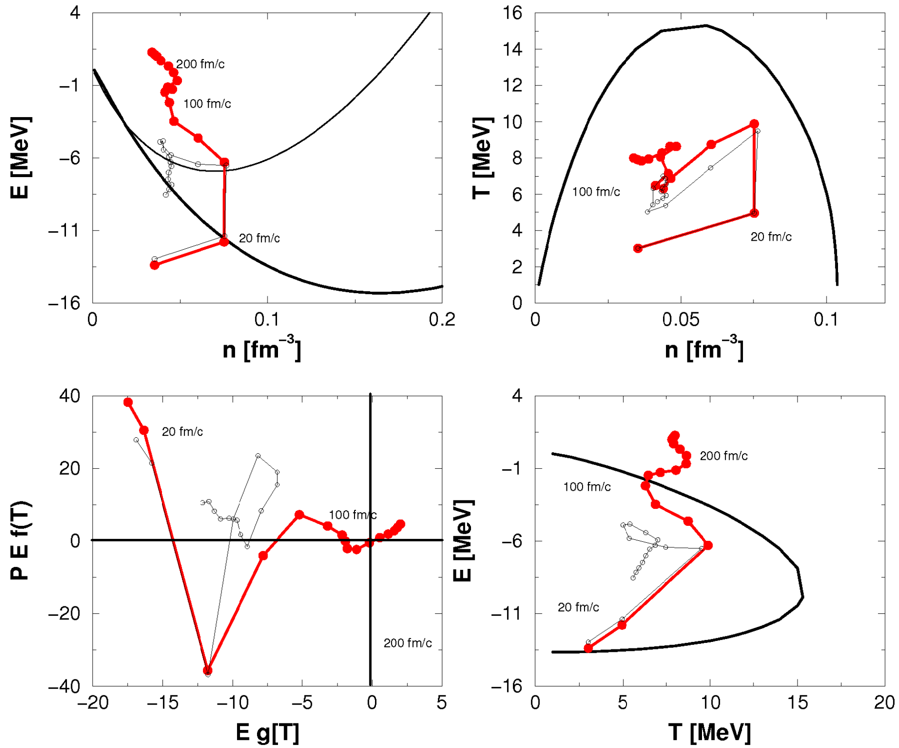

33MeV

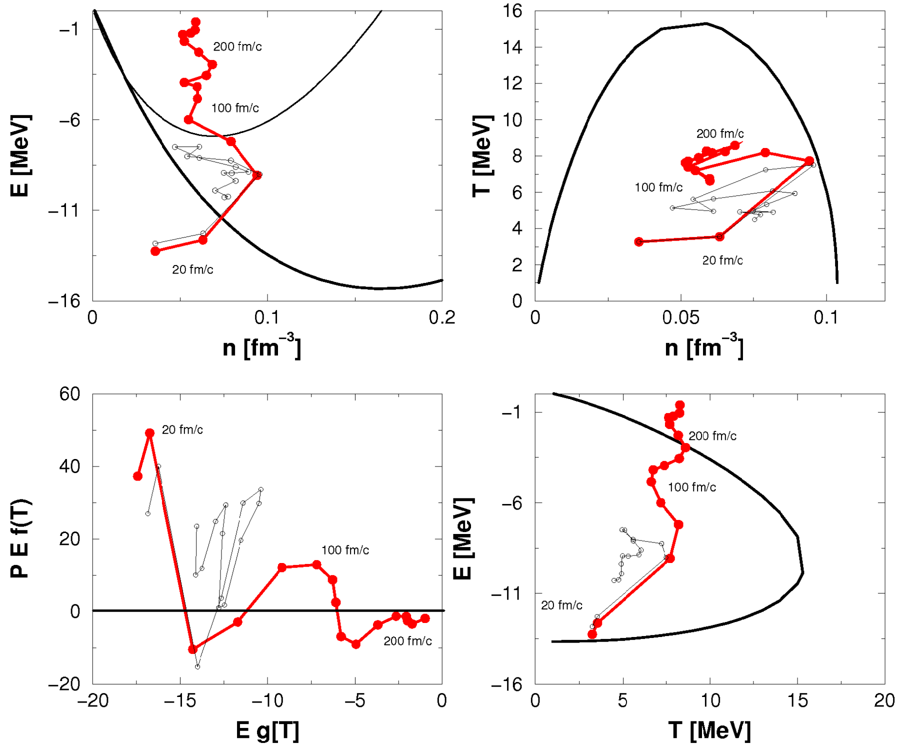

^{56}Ni on ^{179}Au

Summary and prediction

- Nonlocal kinetic theory different nonequilibrium thermodynamics compared to BUU
- Two mechanisms of instability, exp.: H. Ngo et al. 1993 and TAPS Y. Schutz and et. al., Nucl. Phys. A 622, 404 (1997)
  simulation results: surface compression and spinodal decomposition
- Predictions for reactions:

E[MeV]	25	33	50
${}^{58}_{28}$Ni + ${}^{197}_{79}$Au	S	C S	C (S)
${}^{129}_{54}$Xe + ${}^{119}_{50}$Sn	C S	C (S)	C

E[MeV]	15	33	60
${}^{157}_{64}$Gd + ${}^{238}_{92}$U	–	C S	C
${}^{181}_{73}$Ta + ${}^{197}_{79}$Au	C S	C (S)	C

- Fast surface eruption happens outside spinodal region
- For higher energies there is not enough time to rest at the spinodal, system decays before
- Prediction nicely confirmed by Δ-scaling of INDRA data
  R. Botet et al., Phys. Rev. Let. 86, 3514 (2001)
- Nonlocal extension of BUU describes enhancement of high energetic spectra of protons and the midrapidity charge distribution better
- Flow calculations by nonlocal BUU in better agreement with data (under preparation)